Original Article

Measurement of missing video frames in NPP control room monitoring system using Kalman filter

Mrityunjay Chaubey [a], Lalit Kumar Singh [b], Manjari Gupta [a, *]

[a] Computer Science, Centre for Interdisciplinary Mathematical Sciences, Institute of Science, Banaras Hindu University, Varanasi, 221005, India
[b] Department of Computer Science & Engineering, IIT (BHU), Varanasi, India

A R T I C L E   I N F O

A B S T R A C T

Using the Kalman filtering technique, we propose a novel method for estimating the missing video frames to monitor the activities inside the control room of a nuclear power plant (NPP). The purpose of this study is to reinforce the existing security and safety procedures in the control room of an NPP. The NPP control room serves as the nervous system of the plant, with instrumentation and control systems used to monitor and control critical plant parameters. Because the safety and security of the NPP control room are critical, it must be monitored closely by security cameras in order to assess and reduce the onset of any incidents and accidents that could adversely impact the safety of the NPP. However, for a variety of technical and administrative reasons, continuous monitoring may be interrupted. Because of the interruption, one or more frames of the video may be distorted or missing, making it difficult to identify the activity during this time period. This could endanger overall safety. The demonstrated Kalman filter model estimates the value of the missing frame pixel-by-pixel using information from the frame that occurred in the video sequence before it and the frame that will occur in the video sequence after it. The results of the experiment provide evidence of the effectiveness of the algorithm.

1. Introduction

ndustrial automation systems of NPP play a crucial role in monitoring and controlling critical process parameters and ensuring the overall safety of the plant [1,2]. NPP rely on systems to conduct routine inspections and monitoring of the key components of the reactor in order to assess its health and safety. There is an increasing need for more thorough information on inspection and monitoring as power plants get older and their components degrade relative to the early start-of-life settings. The systems and components of NPP systems are regularly monitored and regulated by plant operators to ensure that everything is running as intended. NPP main control room (MCR) has had three generations of design implemented over the course of thirty years. The increased use of computer-based systems to monitor and operate facilities is a significant breakthrough in MCR design [3]. On screens driven by computers, the vast majority of the information has been provided. There is no need for physical components in the "soft" control room, which is used to present and control the plant. An interactive human-system interface (HSI) enabled by video display devices may now monitor and handle most operations in addition to higher computerization levels. Operator activities transition toward knowledge-based activities as analog systems are gradually replaced by digital technologies for routine control and safety operations of NPP. Operator training in the future will be more focused on understanding the system response to system problems. The establishment of effective teams may entail the education of all employees on the roles and duties of their coworkers. Seven of the eight nuclear power plants in UK use Advanced Gas-cooled Reactors (AGR). Around 20% of the country's yearly electricity needs are met by these AGRs. Central to the AGR facility is an enormous control room with hundreds of graphite-brick cylinder pipes at its core. The control rods can be put into these channels, which hold the fuel. Video cameras are among the sensors used in specialized equipment and tools used for inspecting certain fuel routes. The camera collects video of the interior wall of the fuel channel from six different perspectives, some of which overlap with one another, for remote visual inspection (RVI) [4]. Recent years have seen a lot of research and development into the practice of monitoring of the people activities in public or controlled settings for safety or

---

* Corresponding author.
    E-mail addresses: mrityunjay.chaubey11@bhu.ac.in (M. Chaubey), lalit.rs.cse@iitbhu.ac.in (L.K. Singh), manjari@bhu.ac.in (M. Gupta).

security reasons. Surveillance video can be used for a wide range of purposes. For example, the motions and interactions of the persons in the video, as well as the items they carry or leave behind, can all be utilized to detect suspicious activity. By looking at the items, they leave behind or the things they bring with them. In order to monitor a target, a vision camera was utilized by a real-time object tracking system based on vision. It is possible for the monitored object to be one or more in number. It is done by analyzing video frames sequentially to identify and track objects. Background removal algorithm is used to identify moving items in each frame before they may be tracked across many frames. In order to keep track of the moving objects, the tracking algorithm employed the data from the detection stage. However, relying entirely on measurements generated at the detection stage is not safe due to the inefficient algorithm performance or limitations. As a result, the Kalman filtering technique can be altered to adjust for fluctuations and missing measurements whenever the detection stage fails. Based on the identified object's center position and velocity, the missing data is estimated. Jorge, Carlos Alexander F. et al. [5] provide a full explanation of surveillance methods and applications. Video surveillance equipment is used to monitor the NPP control room and look for any indicators of human activity that would impact the safety and security. If for any reason, a single frame of the inspection video is corrupted or disappears during the process of monitoring the control room of the nuclear power plant, the inspection process would be severely impacted. In order to get accurate measurements of the missing or broken frames, it is necessary to have a dependable procedure.

Video monitoring is now widely employed in many other sectors such as industry, science, manufacturing, education, e-conferencing, detective work, crime, medicine, etc. such as to measure physiological parameters like heart rate (HR), respiratory rate (RR), heart rate variability (HRV), blood pressure, and oxygen saturation [6]; to monitor and control modern smart grids to ensure efficient and reliable operation [7]; fabric texture analysis; inspection of automotive rubber profiles; rail heads; length measurement of metallic wire ropes; defect detection of the weld bead; alignment of texture patterns for the design of Japanese kimono cloth [8].

Missing frames in the video are often measured by comparing nearby ones' spatial and temporal information to the missing frames themselves. The missing frames can be identified using a variety of motion estimate techniques. BMME, or block-matching motion estimation, is a popular method for identifying the optimal block match. Search patterns are exploited by the BMME algorithms. Motion information can be recovered from compressed video streams using a variety of techniques. It is possible to disguise errors using relatively simple techniques, such as bi-linear interpolation [9]. These pixels are extrapolated from nearby undamaged pixels to fill in any missing areas. Creating new pixels in space and time from a variety of input frames is the goal of many different video interpolation and extrapolation tasks. Three activities in particular have received a lot of attention in the last few years. The first challenge is termed general video inpainting, and it involves a video that has been provided with random voxels (Spatio-temporal pixels) that need to be filled in with the proper value. Interpolation of one or more frames between two input frames (usually consecutive) is known as frame interpolation. The objective of this task is to count the number of consecutive frames that appear is known as video prediction. The goal is to forecast the appearance of a large number of future frames using a collection of input frames [10]. In addition to motion compensation interpolated frames, another way to estimate forward and backward motion vector fields is to use unidirectional motion estimation. These two interpolated frames are then utilized to form an intermediate frame, and

the accuracy of each pixel is evaluated based on the results of this frame. Finally, some researchers utilize a trilateral filter to denoise the initial estimation and fix any flaws that may have occurred [11]. Environmental monitoring requires the use of the wireless multimedia sensor network or WMSN. The network can be envisioned as a multi-view video system when the sensors are used as cameras. While multi-view videos are being wirelessly transmitted, packet loss is a possibility. When video frames are dropped during transmission, the decoder must employ a frame reconstruction technique to calculate the number of missing pixels. In this circumstance, deep learning-based techniques are used to implement an algorithm for the reconstruction of the lost frame [12]. There are several theories. When utilizing the Bayesian frame-rate-up-conversion technique, the intermediate frame can be calculated using the maximum aposteriori probability method. The intermediate frame can be measured using this technique, which includes both a temporal motion model and a spatial image model in the optimization criterion. The motion model represents the spatial structure of neighboring pixels, while the image model describes the temporal correlation of pixels along motion trajectories. The collection of motion hypotheses is generated by using numerous "ideal" motion trajectories rather than just one. The motion-compensated interpolations obtained by all of these multiple motion hypotheses are adaptively combined according to the reliability of each hypothesis to provide an accurate measurement for the pixels in missing intermediate frames [13]. In this research, we offer a novel method to measure the missing frames, pixel-by-pixel, in a given video file, which records the activity in the NPP control room. The technique entails taking the frames out of the video clip, leaving out part of them, and keeping the rest.

The structure of this manuscript is as follows: Section 2 describes the related work with its advantages and limitations. A short mathematical review of the Kalman filter is given in section 3. Section 4 describes the Kalman filter algorithm, and Section 5 presents the proposed methodology. In Section 6, the validation of the proposed methodology is given in detail. Section 7 brought out the conclusions.

2. Related work

In order to estimate the missing pixels in the frame, decoders are used during the measurement procedure. When B.Yan et al. [9] developed a hybrid frame concealment methodology for H.264/AVC, they addressed the difficulties that emerge from employing pixel-based motion vector estimation. The main disadvantages of this approach are the high computing costs and a need to specify a block matching threshold. In video frame inpainting, Ryan Szeto et al. [10] created a temporally-aware interpolation network. Frame interpolation, video prediction, and generic video inpainting all come together in this study to form a task called video frame inpainting. This strategy can result in hazy images, especially if the camera is moving quickly. Using a trilateral filtering technique, Ci Wang et al. [11] came up with a way to increase the frame rate. Moving the frames of the closest neighbor in both the preceding and subsequent directions using motion vectors measured in between the frames is used in this method to anticipate two interpolated frames. The accuracy of the original interpolated frame and its pixels is then estimated using these two predictions. Once the problematic pixels have been repaired, a trilateral filter is applied to the image to fill in all of the missing pixels. When estimating unidirectional motion, the search approach, block matching criteria, and block size all play an important role. Ting-Lan Lin et al. [12] presented a method based on multilayer perceptron regression for reconstructing missing frames in multi-view films in wireless multimedia sensor networks. In addition, a new inpainting

technique is proposed, which makes use of the optical flow algorithm data as well as frames in the immediate vicinity.

An adaptive fusion of motion-compensated interpolations is proposed by Hongbin Lu et al. [13] to present a multiple hypothesis Bayesian frame rate up-conversion strategies for forecasting the intermediate frame with the highest probability of aposteriori. However, this procedure is more time-consuming than other methods. For video frame interpolation, Wang Shen et al. [14] proposed employing a recurrent network to account for spatial degradations. Longer sequences can not be processed easily because of the lengthy and complicated training procedure that goes along with a recurrent neural network.

Xiaozhang Liu et al. [15] proposed an optical flow estimation-based video frame interpolation method with image inpainting. Based on a combined local and global total variation (CLGTV) optical flow estimate model, the optical flow between input frames is analyzed. They also addressed video frame interpolation and optical flow estimation. After that, the optical flow is employed to create the intermediate frames, which are subsequently displayed. A nonlocal self-similarity between video frames is then used to resolve the pixel loss area in an interpolated frame. These additional frames bring the overall frame count up to the necessary number. A typical problem in optical flow estimation is that it is not always possible to accurately detect fine motion structures, especially in regions with considerable and abrupt displacement fluctuation.

For highly corrupted H.264/AVC videos, Shihua Cui et al. [16] suggested an error concealment model, based on Kalman filtering (KF). This algorithm utilized a modified bilinear motion field interpolation (MFI) method to reconstruct both the missing and unexpected motion vectors (the "minority"). It is possible that an unscented Kalman filter might be used instead of the current framework for videos with non-linear motion since the KF prediction is not dependent on the loss rate.

Avinash Paliwal et al. [17] proposed hybrid imaging system-based deep slow-motion video reconstruction technique. A deep learning system for interpolating video frame data was proposed that made use of a hybrid imaging approach. For the purpose of correcting the loss of temporal information included in the original video, a high frame rate video with the limited spatial resolution was used. This approach was unable to make use of the data in the auxiliary frames because of the poor resolution at which they were collected.

Visual misperception can be eliminated using an efficient temporal error concealment approach (ETEC) developed by Xingang Liu et al. [18]. For H.264/AVC inter-frame decoding, this paper employed four 4 × 4 blocks (HVS). The MV of the lost macroblock (MB) can be reconstructed by interpolating data from nearby undamaged MBs based on geometry and other mathematical techniques. Error detection is improved (EC). Block-matching criteria and a lot of processing are required to use this strategy. Wenbo Bao et al. [19] suggested a method for interpolating video frame data based on motion estimation and compensation-driven neural networks. An adaptive warping layer that integrates optical flow and interpolation kernels have been designed such that target frame pixels can be generated using this layer. Due to the fact that this layer is fully differentiable, it allows the flow and kernel estimation networks to be optimized in tandem. Rather than relying on hand-crafted features, the recommended model uses motion estimation and compensation methodologies to achieve its goals. With global motion compensation, it is impossible to accurately depict moving objects within a frame. The importance of motion estimates at the local level follows directly from this.

Yasuyuki Matsushita et al. [20] came up with a method for completing and deblurring videos. It has been proposed that motion inpainting can be used as a new and effective method for producing stabilized videos. In order to seamlessly patch together images, a technique called motion inpainting enables the transmission of motion into blank portions of the image. Instead of calculating point spread functions, they found a deblurring method that transfers and interpolates sharper pixels from adjacent frames (PSFs). The recommended completion strategy relies on motion inpainting to provide implicit assurances of spatial and temporal coherence. The motion inpainting technique can be used to check for consistency. The smoothness of the extrapolated optical flow ensures the smoothness of the spatial continuity of the image stitch indirectly. Furthermore, optical flow from neighboring frames provides temporal consistency in both static and dynamic areas. A global motion estimate is used in this method, which can yield erroneous findings when a moving item occupies a large section of the image. It is feasible for local motion measurements to be erroneous when dealing with objects that are moving swiftly. When dealing with things moving at high speeds, the limits of measuring local motion might lead to erroneous results.

Yonatan Wexler et al. [21] came up with a model for filling in missing information based on the idea of local structures. To solve the completion problem, it first turns it into a global optimization problem with a clear objective function, and then it creates a new algorithm to solve the problem. The usage of reference examples restricts the number of missing values that can be incorporated into cohesive structures. They employ this cutting-edge technology to create substantial "holes" in video sequences showing dynamic and complex circumstances in terms of space and time. Spatiotemporal patches from other areas of the video are sampled to fill in the gaps while maintaining global spatiotemporal consistency between all of the patches that are located in or around the hole. No attempt is made to merge identical pixels from the same (static) area of the scene in the method provided here. Because of this, video clips and images appear to have been recorded in real-time.

3. A short mathematical review of the Kalman filter

A well-known technique for predicting the state variables of a system, the Kalman filter is applied to make such predictions. Various measurements (collected over time) that have variable degrees of uncertainty [22—25] are used to derive the model of the system. This algorithm was developed in order to solve the more general problem of estimation of state $x \in \mathbf{R}^n$ of a discrete time-controlled process governed by the linear stochastic difference equation:

$$x_{k+1} = A_k x_k + B_k u_k + w_k \tag{1}$$

With measurement $z \in \mathbf{R}^m$ that is

$$z_k = H_k x_k + v_k \tag{2}$$

Here the process noise and the measurement noise are given by the random variables w_k and v_k, respectively. It is assumed that they are independent of each other, and are white with their probability distributions being normal.

i.e.

$$p(w) \sim N(0, Q) \tag{3}$$

$$p(v) \sim N(0, R) \tag{4}$$

The n × n matrix A in the difference equation (1) establishes a relationship between the state of the system at the time step k and the state of the system at the time step k + 1 without the influence

of the process noise or a driving function. The control input $u \in R^l$ is related to the state x by the $n \times l$ matrix B_k. The $m \times n$ matrix H establishes a relationship between the state and the measurement z_k within the context of the measurement equation (2).

Now, we can define $\widehat{x}_k^- \in R^n$ as our apriori state estimate at step k based on our knowledge of the process prior to step k, and $\widehat{x}_k \in R^n$ as our aposteriori state estimate at step k given measurement z_k. $\widehat{x}_k^- \in R^n$ is our apriori state estimate at step k based on the knowledge of the process prior to step k. The apriori and aposteriori estimate errors can thus be defined as the following:

$$\overline{e}_k \equiv x_k - \widehat{x}_k^-, \cdot \text{and} \cdot e_k \equiv x_k - \widehat{x}_k$$

The *apriori* estimate error covariance is then

$$P_k = E\left[\overline{e}_k \overline{e}_k^T\right] \tag{5}$$

And the *aposteriori* estimate error covariance is

$$P_k = E\left[e_k e_k^T\right] \tag{6}$$

To derive the equations of the Kalman filter, we first set out with the objective of finding an equation that computes an aposteriori state estimate $\widehat{x}_k$ as a linear combination of an apriori estimate $\widehat{x}_k^-$ and a weighted difference between an actual measurement z_k and a measurement prediction $H_k \widehat{x}_k^-$. This is demonstrated in equation (7)

$$\widehat{x}_k = \widehat{x}_k^- + K(z_k - H_k \widehat{x}_k^-) \tag{7}$$

The measurement innovation, also known as the residual, is the difference in the equation (7) represented by $(z_k - H_k \widehat{x}_k^-)$. The residual is a measure of the deviation from the predicted measurement $H_k \widehat{x}_k^-$ that exists between the actual measurement z_k and the prediction. If there is no residue, then this indicates that both of these statements are accurate.

Because it results in the lowest aposteriori error covariance, the $m \times n$ matrix K in equation (7) is selected to be the gain or blending factor (6). This minimization can be accomplished by first substituting equation (7) into the above definition for e_k, then substituting that into equation (6), performing the indicated expectations, taking the derivative of the trace of the result with respect to K, setting that result equal to zero, and then solving for K. This procedure can be repeated as many times as necessary to achieve the desired level of minimization. The following is an example of a form of the resulting K that minimizes equation (6):

$$K_k = P_k^- H_k^T \left(H_k P_k^- H_k^T + R_k\right)^{-1}$$

$$= \frac{P_k^- H_k^T}{H_k P_k^- H_k^T + R_k} \tag{8}$$

By looking at equation (8), we can see that the gain K weights the residual more heavily as the measurement error covariance R_k gets closer and closer to zero. Specifically

$$\lim_{R_k \to 0} K_k = H_k^{-1}$$

On the other hand, as the *aposteriori* estimate error covariance P_k^- approaches zero, the gain K weights the residual less heavily. Specifically

$$\lim_{P_k^- \to 0} K_k = 0$$

Another way of thinking about the weighting by K is that as the measurement error covariance R_k approaches zero, the actual measurement z_k is trusted more and more, while the predicted measurement $H_k \widehat{x}_k^-$ is trusted less and less. On the other hand, as the *apriori* estimate error covariance P_k^- approaches zero the actual measurement z_k is trusted less and less, while the predicted measurement $H_k \widehat{x}_k^-$ is trusted more and more [26].

4. Kalman filter algorithm

The Kalman filter is a method for estimating a process that makes use of feedback control. Specifically, it makes an estimate of the state of the process at a particular time and then takes input in the form of (noisy) measurements. As a consequence of this, the equations used by the Kalman filter can be broken down into two categories: time update equations and measurement update equations. In order to generate a priori estimates for the subsequent time step, the time update equations are responsible for projecting the current state and error covariance estimates ahead (in time). The measurement update equations are responsible for handling the feedback, which refers to the process of including a new measurement in the a priori estimate in order to obtain an improved *aposteriori* estimate. The equations used to update the time can also be referred to as predictor equations, while the equations used to correct the measurements can be called corrector equations. In point of fact, as can be shown in Fig. 1, the ultimate method of estimation is rather similar to a predictor-corrector approach to the resolution of numerical issues.

The specific equation for the time and measurement updates is given below.

Time update equations

$$\widehat{x}_{k+1}^- = A_k \widehat{x}_k + B_k u_k \tag{9}$$

$$P_{k+1}^- = A_k P_k A_k^T + Q_k \tag{10}$$

Measurement update equations

$$K_k = P_k^- H_k^T \left(H_k P_k^- H_k^T + R_k\right)^{-1} \tag{11}$$

$$\widehat{x}_k = \widehat{x}_k^- + K(z_k - H_k \widehat{x}_k^-) \tag{12}$$

$$P_k = (I - K_k H_k) P_k^- \tag{13}$$

During the initial phase of the measurement update, the Kalman gain is calculated. It is important to note that equation (11) is exactly the same as equation (8). The following step is to take
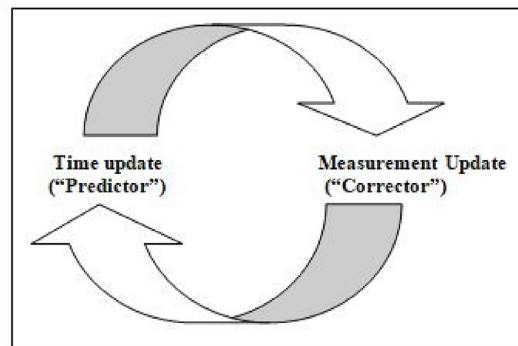

Fig. 1. Kalman filter cycle.

measurements of the procedure in order to get it, and then develop a *aposteriori* state estimate by factoring in the measurements using the equation (12). For the sake of completeness, equation (12) is just a repetition of equation (7) here. Calculating an *aposteriori* error covariance estimate is the final stage, and it may be done with the help of equation (13).

5. Proposed methodology

To estimate the missing frames in an NPP control room monitoring video, we offer a new pixel-by-pixel Kalman filter algorithm that we devised. The method's flowchart is shown in Fig. 2, and the algorithm is detailed in Table 1. Kalman filter is well-suited to systems that are subject to rapid evolution. When it comes to real-time and embedded systems, they are ideal since they are light on memory because they do not need to maintain any history other than the prior state.

Let us have a video signal represented by: $x[n_1, n_2, k]$, where n_1 and n_2 are the spatial coordinates, and k is the temporal component. After the completion of the video capturing process, each frame is extracted. Let there are n frames, denoted by $f_1, f_2, \ldots\ldots, f_n$. The following three frames, from the extracted frames, f_1, f_2 and f_3, are considered for this analysis as shown in Fig. 3. The content of the frame f_2 has been removed on purpose. A new video is now obtained, in which one frame is missed. Using the frames that came before and after it, f_1 and f_3, respectively, the Kalman filter is utilized to measure the value of the missing frame f_2. In addition, the following model is implemented by the application of the Kalman filter in order to measure the missing frame. Using the state transition equation (9), we model the transition of the pixels from the previous frame to the next frame or from the next frame back to the previous frame. Our observed frame is the frame at time k that was measured beforehand, and the observation model is represented by equation (2). The weight that is attributed to the measurements and the current-state estimate is referred to as the Kalman-gain, and it is something that may be "tuned" in order to attain specific performance. When the gain of the filter is high, the most recent measurements are given more weight, and as a result, the filter adapts to them more quickly. In accordance with our methodology, the Kalman gain can be computed by equation (11). With the assistance of Kalman gain, we are able to measure the output using the missing frame by equation (12). Following the computation of the measured frame, an update to the error covariance is performed utilizing equation (13).

6. Validation of the proposed methodology

We conduct our experiments using the MATLAB video file titled "NPP_C.mp4″, which has a total of 209 frames. This is done so that

Table 1
Proposed algorithm.

| Input	:	Video signal $x[n_1, n_2, k]$
Step-1	:	**Extract the frames**
Step-2	:	**Select three consecutive frames f_1, f_2 and f_3**
Step-3	:	**Delete frame f_2 ;**
		Estimation of retrieved frame using Kalman filter
Step-4	:	**Initialize state**
		Initialize error covariance $p = 0$
		Initialize the Gaussian measurement noise R
		Initialize Gaussian process noise Q
		*for $j = 2$: **number of rows***
		*for $k = 2$: **number of columns***
		for $f = 2$: 2 do
		Calculate the previous frame $f - 1$
		Calculate the Kalman gain
		$K_k = \dfrac{p}{p + R}$
		Calculate the retrieved frame
		$\hat{x}_k = \hat{x}_k^- + K_k(Z_k - H\hat{x}_k^-)$
		Calculate the updated error covariance
		$P_k = (1 - K_k)P_k^- + Q$
		endfor
		end for
		end for
Output	:	**Retrieved frame**
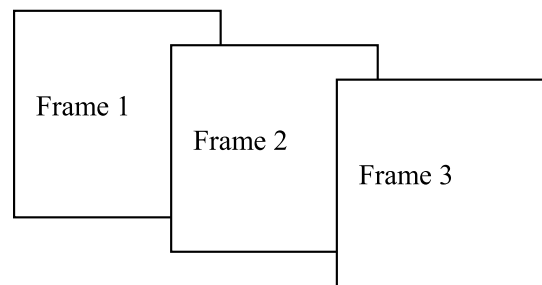
Fig. 3. Three consecutively selected frames.

we can verify that the suggested approach is effective. In MATLAB, we read a video file that was downloaded from Google by using the VideoReader function, which in turn returns a VideoReader object. The object property can be utilized to access a variety of video-related details, including the duration, number of frames, frame rate, and so on. Now we take every single frame from the video and extract it, but we only take the three frames that come immediately after each other as seen in Fig. 4. The selected frames have a dimension of $720 \times 1280 \times 3$ uint.

The second frame from the selected frames is deleted. Fig. 5 shows the missing frame. Our objective is to measure the missing frame.

In order to measure the missing frame, we utilize the Kalman filter with an initial error covariance of zero, the prior frame as the initial state, Gaussian measurement noise with a R value of 2^{-3}, and Gaussian noise process with a Q value of 2^{-6}. The measured portion of the lost frame is depicted in Fig. 6. The numerous aspects of performance are broken down in Table 2 below. For the purpose of conducting a quantitative performance evaluation of the suggested procedure, we computed four performance evaluation parameters. The outcomes are as described below:

6.1. Structural similarity index

The structural similarity index, often known as SSIM, is a perceptual metric that assesses the deterioration in image quality
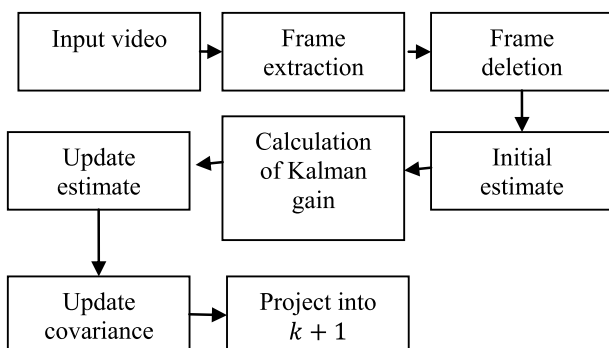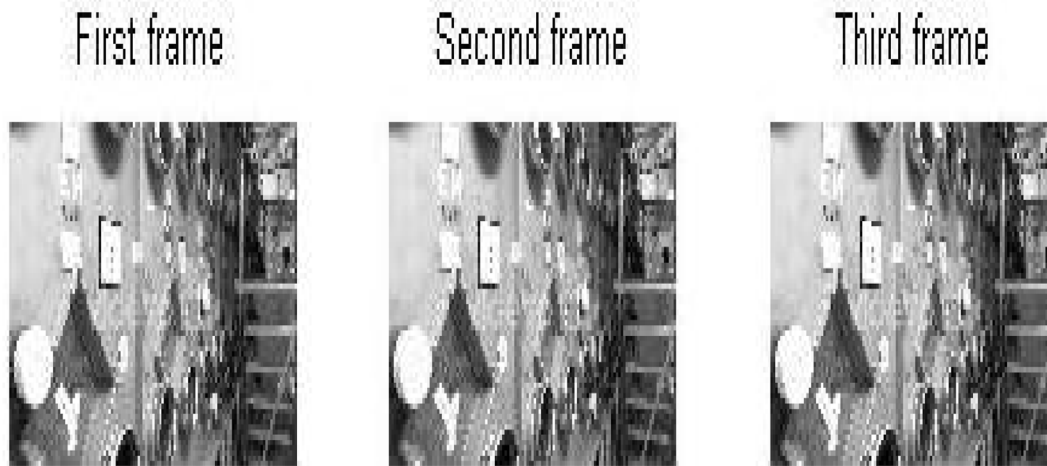

Fig. 2. Flow chart of the proposed methodology.

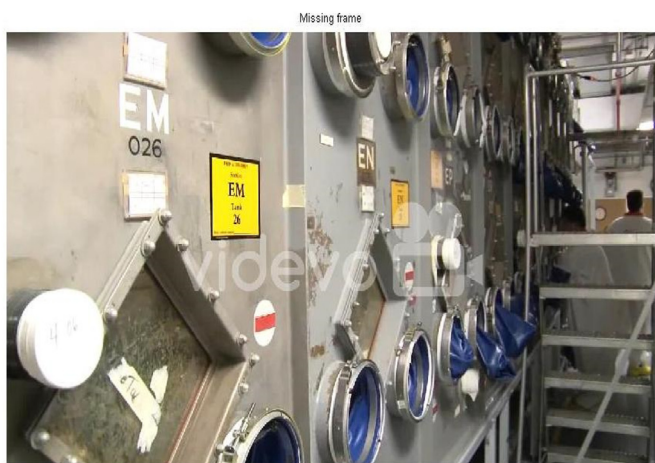**Fig. 4.** Three consecutively selected frames.

Fig. 5. Missing frame.

Fig. 6. Retrieved frame.

Table 2
Performance evaluation metrics.

Performance evaluation parameters	Minimum	Maximum
SSIM	0.9760	0.9760
PSNR	37.8856dB	37.8856dB
Coefficient of correlation	0.9988	1
Error	0.9548%	1.6166%
Sum of squared difference (SSD)	212300756	212300756

to 1, the image quality is considered to be higher.

6.2. Peak signal-to-noise ratio

The peak signal-to-noise ratio (PSNR) of two images can be calculated using the PSNR and expressed in decibels. The quality of the image can be determined by comparing the original image to a compressed or recovered version of the image using this ratio. As the PSNR value goes up, the image's quality, whether it was compressed or recovered, gets better. The PSNR ought to be as high as is practicable. Regarding our situation, the value of PSNR is determined to be 37.8856dB.

6.3. Mean squared error

The difference between the retrieved image and the original image, measured in terms of the mean squared error, is referred to as the mean square error (MSE). The mean square error can be used in a number of different ways to quantify the differences that can exist between the values that are inferred by an estimate and the actual quality that is being certified. The mean squared error, or MSE, is a risk function that represents the expected value of the squared error. When calculating the MSE, which stands for the mean squared error, one must take into account both the variance and the bias of the estimate. If the MSE value is smaller, the result is considered to be of higher quality, but if the MSE value is larger, the result is considered to be of worse quality. Within the framework of the algorithm that we have suggested, the minimum value of MSE is 0.9548 % and the highest value is 1.6166 %.

6.4. Correlation

Correlation is a method for determining the degree of

that occurs as a result of processing, such as the compression of data or the loss of data during transmission. It is a full reference metric that requires two images, a reference image and a processed image from the same image capture. These images must come from the same image capture. In the algorithm that we have proposed, the value of SSIM is calculated to be 0.9760. When the SSIM is closer
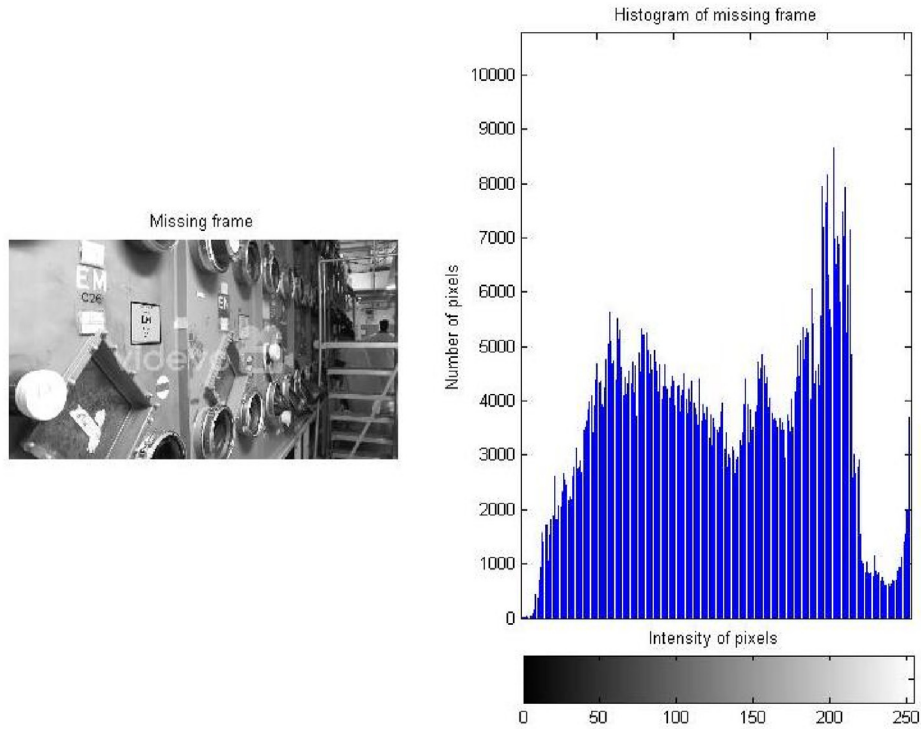
Fig. 7. Missing frame and its equivalent histogram.

probability that two measured quantities have a linear relationship. It is denoted by r and can be calculated as follows:

$$r = \frac{\sum_i (x_i - x_m)(y_i - y_m)}{\sqrt{\sum_i (x_i - x_m)^2}\sqrt{\sum_i (y_i - y_m)^2}}$$

Where x_i and y_i are intensity values of ith pixel in the first and second frames respectively. Also x_m and y_m are mean intensity values of the first and second image respectively. If two images are identical, the correlation coefficient is r = 1, r = 0 if they are fully uncorrelated, and r = −1 if they are completely anti-correlated. Our proposed algorithm gives the minimum and maximum correlation coefficients of 0.9988 and 1, which indicates a good correlation between the deleted frame and the retrieved frame.
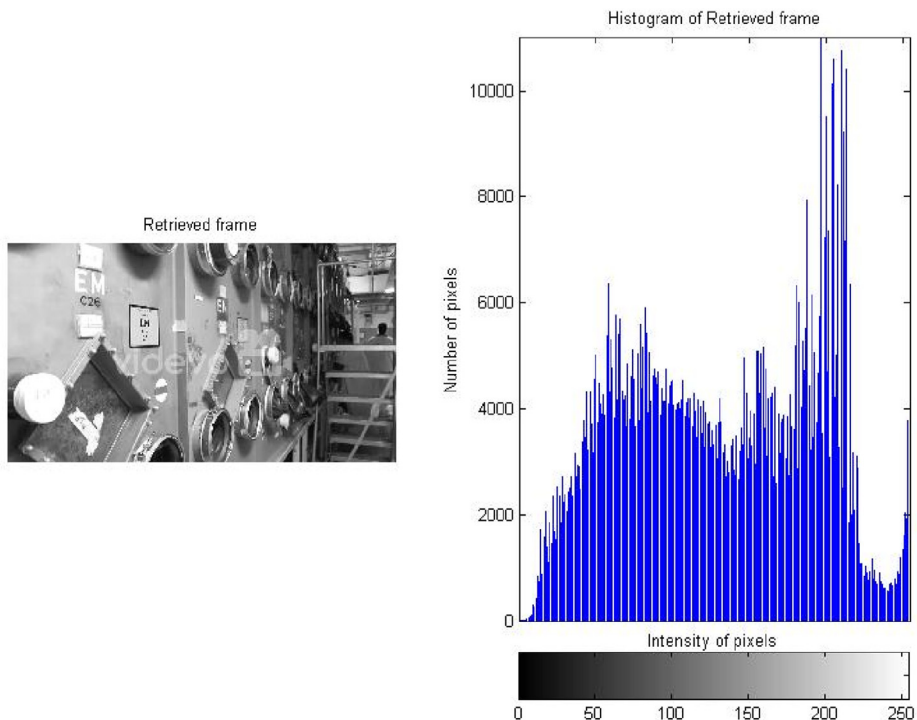

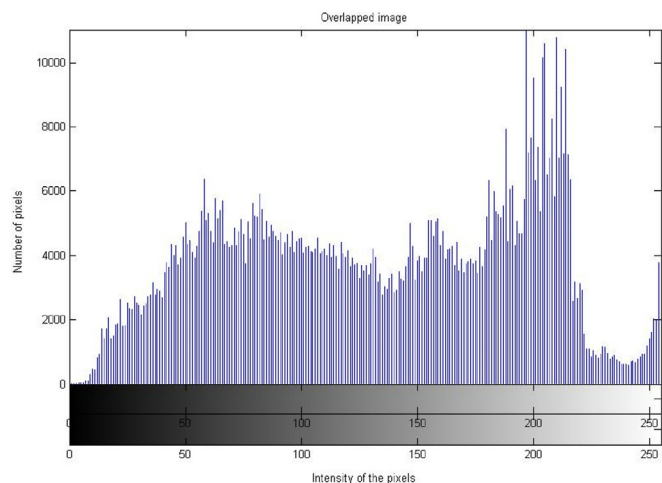**Fig. 8.** Retrieved frame and its equivalent histogram.

Fig. 9. Overlapped histogram of the missing frame and retrieved frame.

6.5. Histogram comparison

A histogram comparison of the missing frame and the retrieved frame is shown in Fig. 7 and Fig. 8 respectively. In addition, we plotted the overlap between both of the histograms in order to visualize the resemblance between the frame that was lost and the frame that was retrieved which is shown in Fig. 9. The sum of the square difference (SSD) between the missing frame and the retrieved frame is (212300756).

7. Conclusion

In this paper, we offer a new method for determining the video frame that is missing from a video. To ensure the safety and security of the NPP control room, it is essential to adopt this kind of video surveillance monitoring. Using a video file of the NPP control room, we begin by selecting three consecutive frames. Our solution is demonstrated by removing the center frame of the video. Using the frames that came before and after it, we may make an educated guess at the estimation of the missing frame in the last stage of the process. We use a technique called Kalman filtering. The previous frame is used as the initial state in this approach, the initial error covariance is assumed to be zero, and both initial Gaussian measurement noise and Gaussian process noise are assumed to be present. The error covariance is likewise assumed to be zero at the start of the procedure using this method. As a result, it generates iterative estimates of the missing frame using Kalman filtering. The outcomes of the experiments support the validity of the methodology that was proposed.

Declaration of competing interest

The authors declare that they have no known competing financial interests or personal relationships that could have appeared to influence the work reported in this paper.

References

[1] Pooja Singh, Lalit Kumar Singh, Modeling and measuring common cause failures in measurement of reliability of nuclear power plant systems, IEEE Transactions on Instrumentation and Measurement 70 (2021) 1—8.

[2] Pooja Singh, Lalit Kumar Singh, Improved measurement accuracy in critical parameters of safety-critical systems WithMultisensor data fusion, IEEE Transactions on Instrumentation and Measurement 70 (2021) 1—8.

[3] Chih-Wei Yang, Tsung-Ling Hsieh, Shiau-Feng Lin, Chiuhsiang Joe Lin, Hui-Ming Teng, Yu-Fang Chiu, Operators' signal-detection performance in video display unit monitoring tasks of the main control room, Safety science 49 (10) (2011) 1309—1313.

[4] Mrityunjay Chaubey, Lalit Kumar Singh, Manjari Gupta, A review of missing video frame estimation techniques for their suitability analysis in NPP, Nuclear Engineering and Technology 54 (April) (2022) 1153—1160.

[5] Jorge, F. Carlos Alexandre, Antonio Carlos A. Mol, Jose M. Seixas, Eduardo Antonio B. Silva, Raphael E. Cota, Bruno L. Ramos, People Detection in Nuclear Plants by Video Processing for Safety Purpose, 2011.

[6] Xun Chen, Juan Cheng, Rencheng Song, Yu Liu, Rabab Ward, Z. Jane Wang, Video-based heart rate measurement: recent advances and future prospects, IEEE Transactions on Instrumentation and Measurement 68 (10) (2018) 3600—3615.

[7] Luisa HB. Liboni, Maurício C. de Oliveira, Ivan N. da Silva, Optimal kalman estimation of symmetrical sequence components, IEEE Transactions on Instrumentation and Measurement 69 (11) (2020) 8844—8852.

[8] Du-ming Tsai, Yi-chun Hsieh, Machine vision-based positioning and inspection using expectation—maximization technique, IEEE Transactions on Instrumentation and Measurement 66 (11) (2017) 2858—2868.

[9] Bo Yan, Hamid Gharavi, A hybrid frame concealment algorithm for H. 264/AVC, IEEE Transactions on Image Processing 19 (1) (2009) 98—107.

[10] Ryan Szeto, Ximeng Sun, Kunyi Lu, Jason J. Corso, A temporally-aware interpolation network for video frame inpainting, IEEE Transactions on Pattern Analysis and Machine Intelligence 42 (5) (2019) 1053—1068.

[11] Ci Wang, Lei Zhang, Yuwen He, Yap-Peng Tan, Frame rate up-conversion using trilateral filtering, IEEE Transactions on Circuits and Systems for Video Technology 20 (6) (2010) 886—893.

[12] Ting-Lan Lin, Hua-Wei Tseng, Yangming Wen, Fu-Wei Lai, Ching-Hsuan Lin, Chuan-Jia Wang, Reconstruction algorithm for lost frame of multiview videos in wireless multimedia sensor network based on deep learning multilayer perceptron regression, IEEE Sensors Journal 18 (23) (2018) 9792—9801.

[13] Liu Hongbin, Ruiqin Xiong, Debin Zhao, Siwei Ma, Wen Gao, Multiple hypotheses Bayesian frame rate up-conversion by adaptive fusion of motion-compensated interpolations, IEEE transactions on circuits and systems for video technology 22 (8) (2012) 1188—1198.

[14] Wang Shen, Wenbo Bao, Guangtao Zhai, Li Chen, Xiongkuo Min, Zhiyong Gao, Video frame interpolation and enhancement via pyramid recurrent framework, IEEE Transactions on Image Processing 30 (2020) 277—292.

[15] Xiaozhang Liu, Hui Liu, Yuxiu Lin, Video frame interpolation via optical flow estimation with image inpainting, International Journal of Intelligent Systems 35 (12) (2020) 2087—2102.

[16] Shihua Cui, Huijuan Cui, Kun Tang, An effective error concealment scheme for heavily corrupted H. 264/AVC videos based on Kalman filtering, Signal, Image and Video Processing 8 (8) (2014) 1533—1542.

[17] Avinash Paliwal, NimaKhademi Kalantari, Deep slow motion video reconstruction with hybrid imaging system, IEEE Transactions on Pattern Analysis and Machine Intelligence 42 (7) (2020) 1557—1569.

[18] Xingang Liu, Laurence T. Yang, Wei Zhu, Kwanghoon Sohn, Efficient temporal error concealment algorithm for H. 264/AVC inter frame decoding, International Journal of Communication Systems 24 (10) (2011) 1282—1297.

[19] Wenbo Bao, Wei-Sheng Lai, Xiaoyun Zhang, Zhiyong Gao, Ming-Hsuan Yang, Memc-net: motion estimation and motion compensation driven neural network for video interpolation and enhancement, IEEE transactions on pattern analysis and machine intelligence 43 (3) (2019) 933—948.

[20] Yasuyuki Matsushita, Weina Ge EyalOfek, Xiaoou Tang, Heung-Yeung Shum, Full-frame video stabilization with motion inpainting, IEEE Transactions on pattern analysis and Machine Intelligence 28 (7) (2006) 1150—1163.

[21] Yonatan Wexler, Eli Shechtman, Michal Irani, Space-time completion of video, IEEE Transactions on pattern analysis and machine intelligence 29 (3) (2007) 463—476.

[22] Michael Rucci, Russell C. Hardie, Kenneth J. Barnard, Computationally efficient video restoration for Nyquist sampled imaging sensors combining an affine-motion-based temporal Kalman filter and adaptive Wiener filter, Applied optics 53 (13) (2014) C1—C13.

[23] Jesse Scott, Michael A. Pusateri, Duane Cornish, Kalman Filter Based Video Background Estimation, 2009 IEEE Applied Imagery Pattern Recognition Workshop (AIPR 2009), IEEE, 2009.

[24] Shigeki Takahashi, Takahiro Ogawa, Haseyama Miki, Restoration Method of Missing Areas in Video Images Using Kalman Filter, 2007. International Conference on Kansei Engineering and Emotion Research.

[25] Alessandro Ferrero, Harsha VardhanaJetti, Simona Salicone, The possibilistic kalman filter: definition and comparison with the available methods, IEEE Transactions on Instrumentation and Measurement 70 (2020) 1—11.

[26] Gary Bishop, Greg Welch, Proc of SIGGRAPH, Course, An Introduction to the Kalman Filter, vol. 8, 2001, p. 41, 27599-23175.